High-Velocity Friction Modeling
for the System with Unbalanced Rotating Mass

Piotr Dutkiewicz, Przemysław Herman, and Maciej Michałek

Chair of Control and Systems Engineering
Poznań University of Technology
Piotrowo 3a, 60-965 Poznań, Poland
{piotr.dutkiewicz/przemyslaw.herman/maciej.michalek}@put.poznan.pl

Abstract. The paper presents the physically motivated derivation of the alternative high-velocity steady-state friction models for the mechanical link-drive rotating system with the mass unevenly distributed around an axis of rotation. Proposed modeling approach reveals the substantial friction nonlinearities which are usually not taken into account in the widely accepted high-velocity friction models in the literature. Friction phenomena arising due to the mass unbalancing are analyzed for two cases of motion with respect to the gravity vector: perpendicular and parallel.

1   Introduction

Friction is an unavoidable and complicated practical phenomenon present in industrial drives. Good model of friction is very valuable for control purposes, since it can be used in model-based control schemes to improve control quality. It is now a frequent control practice to compensate (at least partially) for friction in feedback or feed-forward path. Many practical applications and laboratory results confirm its usefulness. The most serious problems indicated in the literature concern the friction modeling for very low velocities of motion (in the so-called *presliding stage*), where such phenomena like *stick-slip*, hysteresis or compliant micro-displacements are considered (see the review articles [1,2]). On the other hand, for sufficiently high velocities (in the so-called *sliding stage*) it is frequently assumed, that the friction model takes a linear function form of a system velocity (the so-called *viscous friction*). Such a model is often proposed both for systems with the mass evenly distributed around the rotation axis as well as for systems with unbalanced inertia. We will show in the sequel that for systems consisting of the unevenly distributed rotating mass it is in general theoretically not justified modeling approach. It will be presented that for high velocities the steady-state relation between velocity and a friction torque can get a third-order progressive polynomial form or a highly nonlinear position-dependent function. This phenomenon seems to be important in the case of robot manipulators with revolute joints (especially for ones with direct drives), for which the mass of particular rotating links usually is not evenly distributed either due to the design reasons or due to the robot tip load existence.

Different friction models with a nonlinear relation between the generalized friction force f and the high velocity v were proposed in the literature for the single-drive systems. Proposed nonlinear models often consider either the degressive character of the

friction curves by introducing rational powers of velocity [6], the geometry of application [8] or the drag friction component proportional to the second power of velocity [4]. However, these propositions usually comes rather from experimental modeling arguments and do not follow the theoretical analysis of the friction phenomena [3, 6, 8]. Moreover, the proposed friction models are applied to many different motion systems with no consideration of such an important feature as the geometrical mass distribution of the moving parts. The fact that friction depends, apart from the velocity, also on the mechanism position, acceleration or the external load has been indicated in some papers (see [1, 4, 5, 7, 9]), however the theoretical explanation of those problems seems to has not sufficient reflection in the literature.

The aim of the paper is to derive the alternative high-velocity steady-state friction models for the drive-link mechanical system where the link mass is not evenly distributed around the axis of rotation. We will constraint our analysis of friction to the steady state condition which should be understood hereafter as a constant velocity condition of the link/drive (angular acceleration equal to zero). We try to investigate the friction phenomena resulted directly from the rotation of the unbalanced link mass. The analysis will help to claim why and when simpler friction models (like a linear one) are sufficient and when the more complicated nonlinear friction relations are more adequate. We will formally derive the steady-state friction models for a link-drive system for two cases (denoted further as C1 and C2), where the gravity vector is perpendicular (C1) or parallel (C2) to the motion plane.
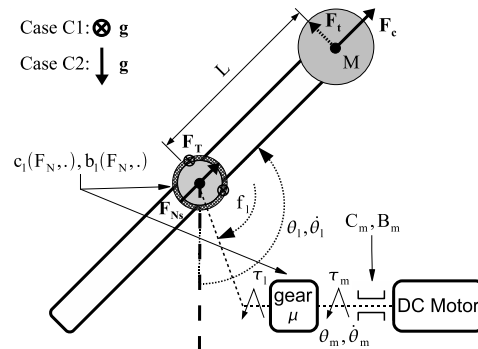

Fig. 1. Single rotating link with the unbalanced mass M

2   Problem statement

Let us consider the single rotating link with the unbalanced mass M connected by a reduction gear with a DC motor drive as depicted in Fig. 1. Assuming, that the armature induction of the motor can be neglected, the equations which describe the system

dynamics can be formulated as follows:

$$J_m \ddot{\theta}_m + f_m = \tau_m - \mu \tau_l \tag{1}$$

$$\tau_m = k_i\, i = \frac{k_i}{R}(u - k_\varepsilon \dot{\theta}_m) \tag{2}$$

$$\mu \triangleq \frac{\theta_l}{\theta_m} = \frac{\dot{\theta}_l}{\dot{\theta}_m} = \frac{\ddot{\theta}_l}{\ddot{\theta}_m} < 1 \qquad \text{and} \qquad \tau_l = J_l \ddot{\theta}_l + f_l + G(\theta_l)\,, \tag{3}$$

where particular elements have the following physical interpretation: J_m, J_l – mass moments of a motor and a link around particular axes of rotation, k_i, k_ε – motor constants, R – motor armature resistance, i – motor armature current, μ – gear ratio, f_m, f_l – friction torques in a motor bearings and in a link joint (together with a transmission), G – gravitational torque, u – motor armature voltage, θ_m, θ_l – angular positions of a motor and a link, τ_m, τ_l – input torques of a motor and a link, respectively.

Using eqs.(2)-(3) in eq.(1) leads, after ordering, to the dynamic model of the considered system expressed on the motor side:

$$(J_m + \mu^2 J_l)\ddot{\theta}_m + G(\theta_m) + F = \frac{k_i}{R}\,u \tag{4}$$

where

$$G(\theta_m) = \mu M g L \sin(\mu \theta_m) \tag{5}$$

$$F = f_m + \mu f_l + \frac{k_i k_\varepsilon}{R}\dot{\theta}_m. \tag{6}$$

Parameter M in eq.(5) denotes the mass of the unbalanced part of a rotating link mounted in the distance L form the axis of rotation (see Fig. 1). The term g is a norm of the gravity vector projected on the motion plane. From now on we will treat the term F from (6) as a resultant friction torque expressed on the motor side.

The problem we will try to solve in the next sections is to derive the formulas for the steady-state friction term f_l included in eq.(6) for the system with unbalanced rotating mass. It will be shown that the whole term F is a nonlinear function of the motor velocity $\dot{\theta}_m$ and additionally in the case C2 (when $G \not\equiv 0$) also a nonlinear function of the link position θ_l.

The main concept that we propose comes from the postulate of varying friction coefficients as the functions of an unbalanced normal force $\boldsymbol{F}_N$ acting on the axis of rotation (compare Fig. 1). The unbalanced force is a result of the rotation of the unbalanced link mass and is proportional to the instantaneous centrifugal acceleration. As a framework model we choose the static friction model structure composed of Coulomb and viscous friction[1] of the general form:

$$f \triangleq b(F_N, \cdot)\dot{\theta} + c(F_N, \cdot)\,\mathrm{sgn}(\dot{\theta}), \tag{7}$$

where, according to the above postulate, we assume that $b(F_N, \cdot), c(F_N, \cdot)$ are functions of a norm of the normal force $\boldsymbol{F}_N$ exerted on the axis of rotation (note: $F_N = \|\boldsymbol{F}_N\|$).

---

[1] Since we are interested in the friction phenomenon mainly for high velocities, such a model structure is practically justified. For simplicity we also temporarily assume friction symmetry.

For the unbalanced mass rotating with a constant velocity $\dot{\theta}_l$, the normal force $\boldsymbol{F}_N$, as a function of the centrifugal acceleration, is proportional to the squared angular velocity of the rotating link: $F_N \propto (\dot{\theta}_l^2 = \mu^2 \dot{\theta}_m^2)$. Moreover, in the case C2 (parallel gravity vector) the resultant instantaneous acceleration of the link (for the constant link velocity) is a nonlinear combination of centrifugal and gravity terms: $F_N = F_N(\dot{\theta}_m^2, g)$. According to mentioned arguments one can not expect that the high-velocity friction model linear in velocity will be still appropriate in considered cases. However, it is worth to emphasize that in the case of perfectly evenly distributed rotating mass the *classical* high-velocity steady-state friction models remains valid, since all normal forces are perfectly balanced (their vector sum is equal to zero) and do not dynamically influence the friction coefficients.

Detailed formulation of the high-velocity friction models for the both cases C1 and C2 of unbalanced rotating mass will be presented in the next two sections.

3   Friction model for the case C1 – gravity vector perpendicular

If the gravity vector $\boldsymbol{g}$ is perpendicular to the motion plane of the link (Case C1 in Fig. 1 $\Rightarrow$ $G(\theta_m) \equiv 0$ in eq.(5)) the high-velocity steady-state friction phenomenon results from the action of two forces: the *transversal* one $\boldsymbol{F}_T$ which is constant and perpendicular to the motion plane (results from the nonzero mass of the link) and the *normal* force $\boldsymbol{F}_N$ acting along the link as depicted in Fig. 1[2]. Due to the centrifugal effect the resultant force $\boldsymbol{F}_N$ has an effect on the axis of rotation and is a function of the centrifugal acceleration $a_c = L\dot{\theta}_l^2$. For the constant link velocity its norm takes the following value:

$$\| \boldsymbol{F}_N \| = F_N = M \cdot a_c = M \cdot L\dot{\theta}_l^2 = M \cdot L\mu^2 \dot{\theta}_m^2. \tag{8}$$

According to the physical relation defining the friction force as a product of a friction coefficient and a normal force of contact (see [1]), we propose the following friction model (7) written for the link joint:

$$f_l \overset{\Delta}{=} (B_{lN} F_N + B_{lT} F_T)\dot{\theta}_l + (C_{lN} F_N + C_{lT} F_T)\,\mathrm{sgn}(\dot{\theta}_l) =$$
$$\overset{(8)}{=} (B_{lN} M L\dot{\theta}_l^2 + \beta_T)\dot{\theta}_l + (C_{lN} M L\dot{\theta}_l^2 + \gamma_T)\,\mathrm{sgn}(\dot{\theta}_l),$$

where B_{lN}, β_T and C_{lN}, γ_T are constant and positive coefficients. Using the definition (3) one can rewrite above formula in the final form:

$$f_l(\dot{\theta}_m) = B_{lN} M L\mu^3 \dot{\theta}_m^3 + C_{lN} M L\mu^2 \dot{\theta}_m^2\,\mathrm{sgn}(\dot{\theta}_m) + \beta_T \mu\dot{\theta}_m + \gamma_T \mathrm{sgn}(\dot{\theta}_m). \tag{9}$$

The friction model (7) written for the motor bearing can be defined as follows:

$$f_m(\dot{\theta}_m) \overset{\Delta}{=} B_m \dot{\theta}_m + C_m \mathrm{sgn}(\dot{\theta}_m), \tag{10}$$

---

[2] For completeness, the tangential force $\boldsymbol{F}_t$ has been also denoted in Fig. 1, but for the steady-state considered here this term is equal to zero.

where B_m and C_m are the constant and positive coefficients. Now we can substitute (9) and (10) in eq. (6) and write the resultant friction torque $F = F(\dot{\theta}_m)$ for the case C1 as follows:

$$F(\dot{\theta}_m) = \mathcal{F}_3 \dot{\theta}_m^3 + \mathcal{F}_2 \dot{\theta}_m^2 + \mathcal{F}_1 \dot{\theta}_m + \mathcal{F}_0, \tag{11}$$

where

$$\mathcal{F}_3 = \mu^4 B_{lN} ML \qquad\qquad \mathcal{F}_2 = \mu^3 C_{lN} ML \, \mathrm{sgn}(\dot{\theta}_m) \tag{12}$$

$$\mathcal{F}_1 = \mu^2 \beta_T + B_m + \frac{k_i k_\varepsilon}{R} \qquad\qquad \mathcal{F}_0 = (\mu \gamma_t + C_m) \, \mathrm{sgn}(\dot{\theta}_m). \tag{13}$$

If one consider unsymmetrical friction phenomenon for positive and negative angular velocities, the torque $F(\dot{\theta}_m)$ has to be defined as:

$$F(\dot{\theta}_m) = \begin{cases} \mathcal{F}_3^+ \dot{\theta}_m^3 + \mathcal{F}_2^+ \dot{\theta}_m^2 + \mathcal{F}_1^+ \dot{\theta}_m + \mathcal{F}_0^+ & \text{if} \quad \dot{\theta}_m > 0 \\ \mathcal{F}_3^- \dot{\theta}_m^3 + \mathcal{F}_2^- \dot{\theta}_m^2 + \mathcal{F}_1^- \dot{\theta}_m + \mathcal{F}_0^- & \text{if} \quad \dot{\theta}_m < 0, \end{cases} \tag{14}$$

where

$$\begin{aligned} \mathcal{F}_3^+ &= \mu^4 B_{lN}^+ ML, & \mathcal{F}_3^- &= \mu^4 B_{lN}^- ML \\ \mathcal{F}_2^+ &= \mu^3 C_{lN}^+ ML, & \mathcal{F}_2^- &= -\mu^3 C_{lN}^- ML \\ \mathcal{F}_1^+ &= \mu^2 \beta_T^+ + B_m^+ + \frac{k_i k_\varepsilon}{R}, & \mathcal{F}_1^- &= \mu^2 \beta_T^- + B_m^- + \frac{k_i k_\varepsilon}{R} \\ \mathcal{F}_0^+ &= \mu \gamma_t^+ + C_m^+, & \mathcal{F}_0^- &= -\mu \gamma_t^- + C_m^-. \end{aligned}$$

Equation (11) shows the third-order polynomial relation for the high-velocity friction, which can reveal the progressive character which is illustrated in Fig. 2. In the figure, the steady-state velocity-voltage curves have been plotted according to the model described by (4) and (11) for parameter values and computed friction coefficients presented in Table 1. It can be seen that for machines equipped with the gears of high-reduction ratio ($\mu \ll 1$) the coefficients $\mathcal{F}_3$, $\mathcal{F}_2$ and the term $\mu^2 \beta_T$ in $\mathcal{F}_1$ are negligibly small and one can assume that for practically admissible velocity range these components do not contribute substantially the resultant friction torque expressed on the motor side (compare Fig. 2). Also in the case of evenly distributed rotating mass we have $M = 0$ and coefficients $\mathcal{F}_3$ and $\mathcal{F}_2$ vanish not contributing the friction. In all these circumstances one obtain the *classical* linear high-velocity friction model. However, for low-reduction ratios μ and even for small unbalanced mass M the effect of polynomial friction relation is clearly visible on the characteristics in the range of medium and high velocities. We suppose that this effect is especially emphasized in the case of fast motion for rotating mass-unbalanced links equipped with the direct drives where we have $\mu = 1$. In this case the liner model seems to be theoretically unfounded.

4   Friction model for the case C2 – gravity vector parallel

If the link motion plane is parallel to the gravity acceleration vector $\boldsymbol{g}$, the transversal force $\boldsymbol{F}_T$ can be neglected in the friction analysis. Now all accelerations which contribute the friction act in the same plane and must be geometrically combined. Fig. 3

Table 1. Parameter values for the theoretical friction model defined by (6), (9), (10) used for plots in Fig. 2 and obtained coefficients (12)-(13)

Parameter	Value	Parameter	Value
M	0.50 kg	g	9.81 m/s^2
M_l	0.20 kg	C_m	0.0080
L	0.25 m	B_m	0.0004
R	1.00 Ω	C_{lN}, C_{lT}	0.0800
k_i	0.02 Nm/A	B_{lN}, B_{lT}	0.0040
k_e	0.20 Vs/rev		

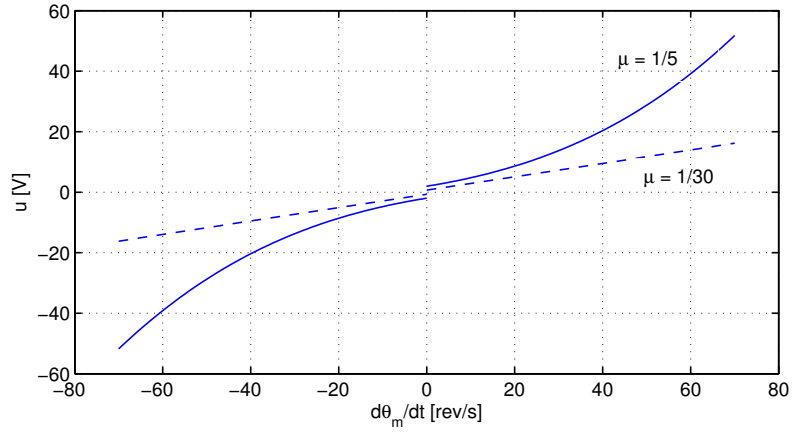| $\mu = 1/5$	$\mu = 1/30$
$\mathcal{F}_3 = +8.0000 \cdot 10^{-7}$	$\mathcal{F}_3 = +6.1728 \cdot 10^{-10}$
$\mathcal{F}_2 = +8.0000 \cdot 10^{-5}$	$\mathcal{F}_2 = +3.7037 \cdot 10^{-7}$
$\mathcal{F}_1 = +4.7139 \cdot 10^{-3}$	$\mathcal{F}_1 = +4.4087 \cdot 10^{-3}$
$\mathcal{F}_0 = \pm 3.9392 \cdot 10^{-2}$	$\mathcal{F}_0 = \pm 1.3232 \cdot 10^{-2}$

Fig. 2. C1: Theoretical polynomial friction model defined by (4) and (11) computed as the steady-state relation between the motor velocity $\dot{\theta}_m$ and the motor armature voltage u for two values of the gear ratio μ

illustrates the situation where two accelerations: gravitational one $\boldsymbol{g}$ and centrifugal one $\boldsymbol{a}_c = \boldsymbol{F}_c/M$ are combined leading to the resultant acceleration $\boldsymbol{a}$ acting on the axis of rotation due to the constant-velocity motion of the unbalanced mass M. The resultant force $\boldsymbol{F}_N$ which contribute the steady-state friction in the link joint is obtained as

$$\boldsymbol{F}_N = M_l\boldsymbol{g} + M\boldsymbol{a}, \tag{15}$$

where $\boldsymbol{a} = \boldsymbol{a}_c + \boldsymbol{g}$, M_l is the mass of the link (without the unbalanced part M) and

$$\boldsymbol{g} = \begin{bmatrix} 0 \\ -g \end{bmatrix}, \ \boldsymbol{a}_c = \begin{bmatrix} L\dot{\theta}_l^2 \sin\theta_l \\ -L\dot{\theta}_l^2 \cos\theta_l \end{bmatrix} \ \Rightarrow \ \boldsymbol{a} = \begin{bmatrix} L\dot{\theta}_l^2 \sin\theta_l \\ -L\dot{\theta}_l^2 \cos\theta_l - g \end{bmatrix}$$

in the coordinate frame $\{x, y\}$ denoted in Fig. 3. In a consequence, the norm of the normal force $\boldsymbol{F}_N$ is velocity and position dependent:

$$F_N(\dot{\theta}_l, \theta_l) = \sqrt{(ML)^2\dot{\theta}_l^4 + 2g(M + M_l)ML\dot{\theta}_l^2 \cos\theta_l + (M + M_l)^2 g^2}. \tag{16}$$
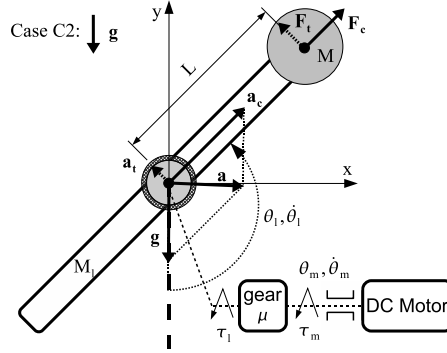
Fig. 3. C2: The link with the unbalanced mass M rotating in the plane of the gravitational acceleration g. Note, that for a constant link velocity condition, the tangential acceleration $a_t \equiv 0$

Now we define the friction torque in the joint link similarly to the proposition from the previous section:

$$f_l = b_l(F_N, \cdot)\dot{\theta}_l + c_l(F_N, \cdot)\,\mathrm{sgn}(\dot{\theta}_l) \stackrel{\triangle}{=} B_{lN}F_N(\dot{\theta}_l, \theta_l)\dot{\theta}_l + C_{lN}F_N(\dot{\theta}_l, \theta_l)\,\mathrm{sgn}(\dot{\theta}_l),$$

where B_{lN} and C_{lN} are constant and positive coefficients, but now the normal force $F_N = F_N(\dot{\theta}_l, \theta_l)$ is additionally a nonlinear function of link position according to (16). Using definition (3) one can express above formula in the terms of motor velocity and motor position as follows:

$$f_l(\dot{\theta}_m, \theta_m) = B_{lN}F_N(\dot{\theta}_m, \theta_m)\mu\dot{\theta}_m + C_{lN}F_N(\dot{\theta}_m, \theta_m)\,\mathrm{sgn}(\dot{\theta}_m),$$

where

$$F_N(\dot{\theta}_m, \theta_m) = \sqrt{(ML)^2\mu^4\dot{\theta}_m^4 + 2g(M + M_l)ML\mu^2\dot{\theta}_m^2\cos(\mu\theta_m) + (M + M_l)^2g^2}.$$
$$(17)$$

Assuming the friction model (10) for the motor bearing we are ready to write the formula describing the resultant friction torque F from eq.(6) for the case C2. We obtain:

$$F(\dot{\theta}_m, \theta_m) = \mathcal{F}_1(\dot{\theta}_m, \theta_m)\dot{\theta}_m + \mathcal{F}_0(\dot{\theta}_m, \theta_m), \tag{18}$$

where

$$\mathcal{F}_1(\dot{\theta}_m, \theta_m) = \mu^2 B_{lN}F_N(\dot{\theta}_m, \theta_m) + B_m + \frac{k_i k_\varepsilon}{R} \tag{19}$$

$$\mathcal{F}_0(\dot{\theta}_m, \theta_m) = \Big(\mu C_{lN}F_N(\dot{\theta}_m, \theta_m) + C_m\Big)\,\mathrm{sgn}(\dot{\theta}_m) \tag{20}$$

with $F_N(\dot{\theta}_m, \theta_m)$ described in (17). For the unsymmetrical friction phenomenon one has to modify the resultant torque $F(\dot{\theta}_m, \theta_m)$ as follows:

$$F(\dot{\theta}_m, \theta_m) = \begin{cases} \mathcal{F}_1^+(\dot{\theta}_m, \theta_m)\dot{\theta}_m + \mathcal{F}_0^+(\dot{\theta}_m, \theta_m) & \text{if} \quad \dot{\theta}_m > 0 \\ \mathcal{F}_1^-(\dot{\theta}_m, \theta_m)\dot{\theta}_m + \mathcal{F}_0^-(\dot{\theta}_m, \theta_m) & \text{if} \quad \dot{\theta}_m < 0, \end{cases} \tag{21}$$

where

$$\mathcal{F}_1^+(\dot{\theta}_m, \theta_m) = \mu^2 B_{lN}^+ F_N(\dot{\theta}_m, \theta_m) + B_m^+ + \frac{k_i k_\varepsilon}{R}$$

$$\mathcal{F}_1^-(\dot{\theta}_m, \theta_m) = \mu^2 B_{lN}^- F_N(\dot{\theta}_m, \theta_m) + B_m^- + \frac{k_i k_\varepsilon}{R}$$

$$\mathcal{F}_0^+(\dot{\theta}_m, \theta_m) = \mu C_{lN}^+ F_N(\dot{\theta}_m, \theta_m) + C_m^+$$

$$\mathcal{F}_0^-(\dot{\theta}_m, \theta_m) = -\mu C_{lN}^- F_N(\dot{\theta}_m, \theta_m) - C_m^-.$$

Let us analyze some interesting properties of derived friction model (17)-(20). Note that the friction nonlinearity results from the nonlinear function $F_N(\dot{\theta}_m, \theta_m)$. Figure 4 illustrates the friction torque (18) as a function of the link angular position $\theta_l \in (0; 2\pi]$ and the link velocity $\dot{\theta}_l \in (0; 8\pi]$ [rad/s]. The plot has been obtained for the gear ratio $\mu = 1/5$ and for the model parameter values included in Table 1.
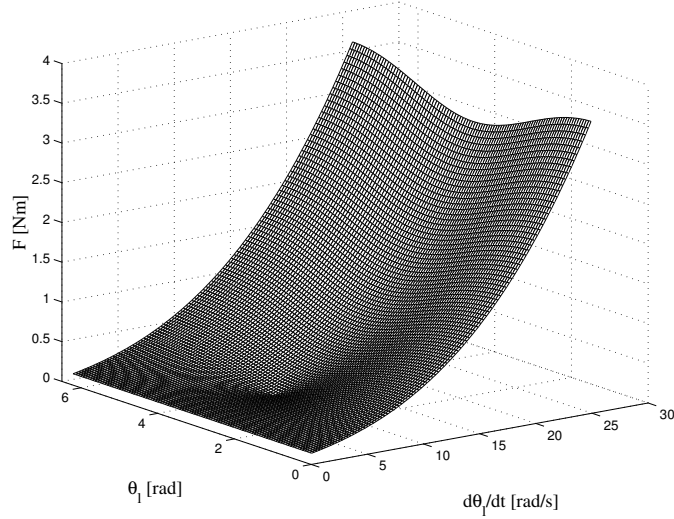

Fig. 4. C2: Friction torque (18) as a function of the link angular position θ_l and the positive link velocity $\dot{\theta}_l$; the global minimum can be seen for $\dot{\theta}_l^* = 7.41$ [rad/s] and $\theta_l^* = \pi$ [rad]

From (16) one can note that F_N is a periodic function of the link position θ_l. It is clear that for every fixed (and constant) link velocity $\dot{\theta}_l = \mu \dot{\theta}_m$ the normal force takes the following extremal values:

$$F_{Nmin} = \left| (M + M_l)g - ML\dot{\theta}_l^2 \right| \quad \text{for} \quad \theta_l = \pi \tag{22}$$

$$F_{Nmax} = \left| (M + M_l)g + ML\dot{\theta}_l^2 \right| \quad \text{for} \quad \theta_l = 0. \tag{23}$$

Hence the resultant friction torque (18) also varies along the full link revolution despite the constant link velocity (see Fig. 4). It is interesting that for the special value of the link velocity

$$\dot{\theta}_l^* = \sqrt{\frac{g(M_l + M)}{ML}}$$

the minimum (22) is equal to zero. In a consequence, for the upper link position the friction torque (18) results only from the motor friction phenomenon. This situation is visible in Fig. 4 as a hollow in the surface (global minimum of the friction torque). Velocity value $\dot{\theta}_l^*$ corresponds to the special centrifugal acceleration $\boldsymbol{a}_c^* = L\dot{\theta}_l^{*2}$ acting on the mass M for which the centrifugal force $\boldsymbol{F}_c^* = M\boldsymbol{a}_c^*$ compensates the weight $\boldsymbol{F}_g = (M_l + M)\boldsymbol{g}$ of the whole rotating system (the link with the unbalanced mass, see Fig. 3). If the link velocity increases over the value $\dot{\theta}_l^*$, the centrifugal force overcompensates the system weight for the link position $\theta_l = \pi$ and in a consequence the value F_{Nmin} becomes greater than zero and continuously increases with velocity (compare Fig. 4). Detailed plots of the friction torque (18) and the normal force (16) are presented in Fig. 5. Three intersections along the velocity axis of the friction surface from Fig. 4 there are presented. Note the non-smooth transition of the normal force F_N (due to the absolute value in (22)) for the velocity $\dot{\theta}_l^* = 7.41$ [rad/s].
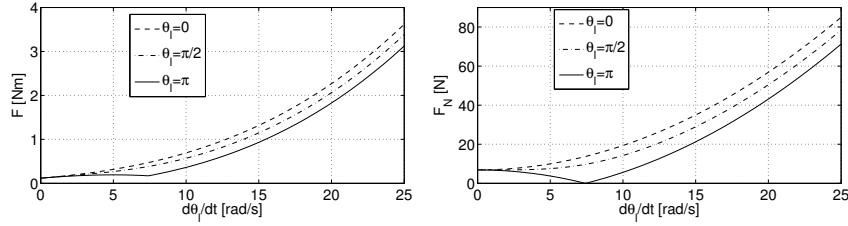

Fig. 5. C2: Friction torque F (18) and the normal force F_N (17) as the functions of the link velocity $\dot{\theta}_l$ computed for three values of the link angle $\theta_l \in \{0, \pi/2, \pi\}$

It is worth to note that for two special angular positions of the link, namely for $\theta_l = 0$ and $\theta_l = \pi$ where the normal force takes the extremal values (22)-(23), the friction torque (18) takes the third-order polynomial form similarly to the friction model from the case C1. It can be easily derived substituting (22) or (23) into (19)-(20) and ordering particular terms. Using (23) one gets the following polynomial for the bottom link position ($\theta_l = \mu\theta_m = 0$):

$$F(\dot{\theta}_m, \theta_l = 0) = \mathcal{F}_{30}\dot{\theta}_m^3 + \mathcal{F}_{20}\dot{\theta}_m^2 + \mathcal{F}_{10}\dot{\theta}_m + \mathcal{F}_{00}, \tag{24}$$

where

$$\mathcal{F}_{30} = \mu^4 B_{lN} ML, \qquad\qquad \mathcal{F}_{20} = \mu^3 C_{lN} ML \operatorname{sgn}(\dot{\theta}_m),$$

$$\mathcal{F}_{10} = \mu^2 B_{lN}(M + M_l)g + B_m + \frac{k_i k_\varepsilon}{R}, \qquad \mathcal{F}_{00} = (\mu C_{lN}(M + M_l)g + C_m)\operatorname{sgn}(\dot{\theta}_m).$$

The polynomial for the upper link position ($\theta_l = \pi$) results from utilizing eq.(22) and it has the form:

$$F(\dot{\theta}_m, \theta_l = \pi) = \mathcal{F}_{3\pi}\dot{\theta}_m^3 + \mathcal{F}_{2\pi}\dot{\theta}_m^2 + \mathcal{F}_{1\pi}\dot{\theta}_m + \mathcal{F}_{0\pi}, \tag{25}$$

where

$$\mathcal{F}_{3\pi} = -s\mu^4 B_{lN} ML, \qquad\qquad \mathcal{F}_{2\pi} = -s\mu^3 C_{lN} ML \, \mathrm{sgn}(\dot{\theta}_m),$$

$$\mathcal{F}_{1\pi} = s\mu^2 B_{lN}(M + M_l)g + B_m + \frac{k_i k_\varepsilon}{R}, \qquad \mathcal{F}_{0\pi} = (s\mu C_{lN}(M + M_l)g + C_m)\,\mathrm{sgn}(\dot{\theta}_m)$$

and

$$s \triangleq \begin{cases} +1 & \text{if} \quad ML(\mu\dot{\theta}_m)^2 < (M + M_l)g \\ -1 & \text{if} \quad ML(\mu\dot{\theta}_m)^2 > (M + M_l)g \end{cases}.$$

5   Remarks and future work

In the authors opinion the high-velocity friction modeling issue has not found enough attention in the literature so far. Simple fact that friction is a function of the normal force $\boldsymbol{F}_N$, which depends on the varying acceleration of the mass-unbalanced rotating system was a motivation of considering the high-velocity friction phenomenon ones again. The derived friction models indicate the substantial nonlinearity in the friction phenomenon (in the form of progressive functions) which can arise for high constant velocities in the mass-unbalanced rotating systems. It must be stressed that since our intention was to focus only on the influence of the unbalanced rotating mass, we have not considered all the practical frictional effects like for instance the drug friction or the temperature influence on the friction coefficients. More complete friction analysis should take into account also these phenomena. It has been shown that for systems with the gears of low-reduction ratios (especially for direct drives) the derived nonlinear effects can not be treated as negligible. Moreover, for the case C2 we have shown that the friction can depend not only on the velocity but also on the instantaneous position of the link. It is worth to note that for the high-reduction ratios of applied transmissions derived nonlinear friction models become the widely accepted linear-in-velocity ones.

The authors believe that models proposed in the paper can explain, at least in part, experimental results concerning the friction effects presented in [3] and [7]. In the near future the experimental testbed will be prepared which will allow to practically validate theoretical friction models proposed in the paper. The extension of the presented analysis to the multi-link serial manipulator case is also planned as the future work.

References

1. B. Armstrong-Hélouvry, P. Dupont, and C. Canudas de Wit. A survey of models, analysis tools and compensation methods for the control of machines with friction. *Automatica*, 30(7):1083–1138, 1994.
2. J. Awrejcewicz and P. Olejnik. Analysis of dynamic systems with various friction laws. *Applied Mechanics Reviews*, 58:389–411, 2005.

3. B. Bona, M. Indri, and N. Smaldone. Nonlinear friction phenomena in direct-drive robotic arms: an experimental set-up for rapid modeling and control prototyping. In *Preprints of the 7th IFAC Symposium on Robot Control*, pages 59–64, Wrocław, 2003.

4. S. S. Ge, T. H. Lee, and S. X. Ren. Adaptive friction compensation of servo mechanisms. *International Journal of Systems Science*, 32(4):523–532, 2001.

5. A. Gogoussis and M. Donath. Coulomb friction joint and drive effects in robot mechanisms. *IEEE*, pages 828–836, 1987.

6. M. Grotjahn, M. Daemi, and B. Heimann. Friction and rigid body identification of robot dynamics. *International Journal of Solids and Structures*, 38:1889–1902, 2001.

7. M. Grotjahn, B. Heimann, and H. Abdellatif. Identification of friction and rigid-body dynamics of parallel kinematic structures for model-based control. *Multibody System Dynamics*, 11:273–294, 2004.

8. H. Olsson, K. J. Åström, C. Canudas de Wit, M. Gäfvert, and P. Lischinsky. Friction models and friction compensation. *European Journal of Control*, (4):176–195, 1998.

9. S. M. Phillips and K. R. Ballou. Friction modeling and compensation for an industrial robot. *Journal of Robotic Systems*, 10(7):947–971, 1993.